Proc. Natl. Acad. Sci. USA
Vol. 85, pp. 8703–8707, November 1988
Neurobiology

M2 δ, a candidate for the structure lining the ionic channel of the nicotinic cholinergic receptor

(synaptic membranes/ionic selectivity/protein structure/planar bilayers/single channels)

SHIGETOSHI OIKI*, WALEED DANHO†, VINCENT MADISON†, AND MAURICIO MONTAL‡§

*Roche Institute of Molecular Biology, Nutley, NJ 07110; †Hoffmann-La Roche Inc., Roche Research Center, Nutley, NJ 07110; and ‡Departments of Biology and Physics, University of California, San Diego, La Jolla, CA 92093-0319

Communicated by Russell F. Doolittle, July 18, 1988 (received for review April 28, 1988)

ABSTRACT **A synthetic 23-mer peptide that mimics the sequence of the putative transmembrane M2 segment of the *Torpedo californica* acetylcholine receptor (AcChoR) δ subunit—Glu-Lys-Met-Ser-Thr-Ala-Ile-Ser-Val-Leu-Leu-Ala-Gln-Ala-Val-Phe-Leu-Leu-Leu-Thr-Ser-Gln-Arg—forms discrete ionic channels in phosphatidylcholine bilayers. In contrast, a synthetic peptide that mimics the sequence of the putative M1 transmembrane segment of the *Torpedo* AcChoR δ subunit—Leu-Phe-Tyr-Val-Ile-Asn-Phe-Ile-Thr-Pro-Cys-Val-Leu-Ile-Ser-Phe-Leu-Ala-Ser-Leu-Ala-Phe-Tyr—does not form channels. The synthetic M2 δ channel peptide exhibits features that are characteristic of the authentic AcChoR channel, such as single channel conductances, discrimination of cations over anions, and channel lifetimes for open and closed states in the millisecond time range. Energetic considerations suggest that an aggregate of five amphipathic α-helices conforms the channel. Thus, the M2 segment may be a component of the AcChoR channel structure.**

The *Torpedo californica* nicotinic acetylcholine receptor (AcChoR) is a complex of five glycoproteins with subunit composition $\alpha_2\beta\gamma\delta$ (ref. 1; reviewed in refs. 2, 3). Analysis of the AcChoR primary structure led to the assignment in each subunit of four hydrophobic transmembrane segments designated as M1, M2, M3, and M4 (4–8), a fifth amphipathic segment known as MA (9–11), a β-strand, or M6, and a seventh amphipathic α-helix, M7 (12, 13). An unsolved issue concerns the identification of specific transmembrane segments that form the channel.

Several key observations suggest that M2 is a likely candidate to be involved in forming the AcChoR pore structure. (*i*) Affinity labeling with noncompetitive channel blockers, such as chlorpromazine (14–16) and triphenylmethylphosphonium (17–19), identified serine 262 in M2 of the δ subunit as a reactive site. (*ii*) Analysis of the single channel conductance (γ) of AcChoRs, expressed in *Xenopus* oocytes, containing chimeric *Torpedo*-bovine δ subunits demonstrated that M2 and the adjacent segment connecting M2 with M3 exert a profound effect on ion conduction through open AcChoR channels (20). (*iii*) Electrophysiological evidence indicates that ionic conduction through open AcChoR channels is consistent with a water-filled channel structure (21–24).

Fig. 1*A* shows the amino acid sequences of the transmembrane M2 segment of the *Torpedo* AcChoR α, β, γ, and δ subunits (refs. 4–8; reviewed in refs. 2, 3). Fig. 1*B* illustrates the sequence of M2 from δ subunits of AcChoRs from *Torpedo* (4–8), chicken (25), mouse (26), and cow (27) (reviewed in ref. 2). Evidently, M2 exhibits high homology between subunits of the *Torpedo* $\alpha_2\beta\gamma\delta$ complex and high evolutionary conservation among different species. Secondary structure predictors suggest that the M2 sequences could form amphipathic α-helices (2, 9–11, 28–32). Five helices may aggregate in the membrane with their hydrophobic surfaces outward and hydrophilic surfaces inward, forming a putative ion channel (2, 3, 9–11, 14–19). These structural considerations suggest that the M2 δ segment may be involved in conforming the pore (14–19).

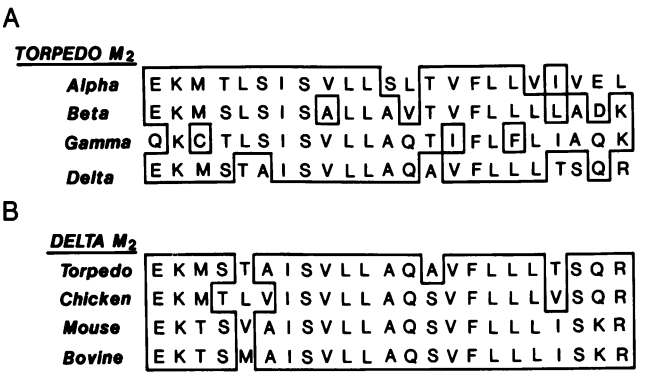

FIG. 1. Amino acid sequences of segments postulated to be involved in AcChoR channel lining. Standard one-letter amino acid code is used. (*A*) Assigned channel segments for the *Torpedo* AcChoR M2 transmembrane segment of the four distinct subunits (4–8). (*B*) M2 segments of AcChoR δ subunits from *Torpedo* (4–8), chicken (25), mouse (26), and calf (27). The synthetic channel peptide corresponds to *Torpedo* AcChoR δ M2 segment (*A* and *B*). The 23-mer α-helix would be ≈35 Å long, a length sufficient to span the lipid bilayer.

We report here a direct test of this notion: A 23-mer peptide corresponding to the sequence of M2 of the *Torpedo* AcChoR δ subunit was synthesized by solid-phase methods (33, 34) and incorporated into lipid bilayers, and its ability to form ionic channels was determined (35). Results lead us to suggest that an aggregate of five amphipathic α-helices may line the AcChoR channel structure; a preliminary account has been presented elsewhere (36).

MATERIALS AND METHODS

Peptide Synthesis and Incorporation into Planar Lipid Bilayers. Peptides were synthesized by solid-phase methods and purified by reversed-phase HPLC (33–35). Peptide purity was confirmed by analytical HPLC, amino acid analysis, and microsequencing. Planar bilayers were formed by hydrophobic apposition of two lipid monolayers initially formed at the air–water interface, and the electrical properties were studied essentially as described (37). Peptides were incorporated into

The publication costs of this article were defrayed in part by page charge payment. This article must therefore be hereby marked "*advertisement*" in accordance with 18 U.S.C. §1734 solely to indicate this fact.

Abbreviations: γ, single channel conductance; AcChoR, acetylcholine receptor; V, applied voltage; τ_o, open channel lifetime; τ_c, closed channel lifetime; PtdCho, 1,2-diphytanoyl-*sn*-glycero-3-phosphocholine.

§To whom reprint requests should be addressed.

FIG. 2. Membrane currents at an applied voltage (V) = 100 mV in PtdCho bilayers containing synthetic M2 δ-mimicking peptide (*A*) and M1 δ-mimicking peptide (*B*). Signals were low-pass filtered at 300 Hz and digitized at 0.6-ms sampling interval. Bilayers were formed across a Teflon septum possessing an aperture of 100 μm (diameter). The aqueous solution was 0.5 M NaCl/5 mM Hepes, pH 7.2. Single channel events with γ = 40 pS are clearly identified in *A* (M2 δ peptide) but not in *B* (M1 δ peptide) under otherwise identical conditions. Upward deflections correspond to channel openings.

bilayers from mixed lipid–peptide monolayers: purified peptide [50 μM in chloroform/methanol (1:1)] was mixed with lipid [1,2-diphytanoyl-*sn*-glycero-3-phosphocholine (PtdCho) was from Avanti, 2 mg/ml in hexane] to achieve final peptide/lipid molar ratios in the range of 1/100–1/10,000. Bilayers were formed across apertures with diameters ranging from 75 μm to 150 μm perforated in a 25-μm-thick Teflon septum separating two 1-ml-capacity Teflon chambers (37). The hole was coated with 2 μl of 0.5% squalene (Sigma) in hexane. All bilayers studied were stable for several hours at 24 ± 1°C and had specific capacitances of 0.7–0.8 $\mu F/cm^2$. Bilayers were also formed at the tip of patch pipets (37) fabricated from Corning Glass 7040 (Garner Glass, Claremont, CA). The conductance of unmodified lipid bilayers was ≤10 pS.

Data Acquisition and Analysis. Electrical recordings and data processing were conducted as described (37, 38). Current was measured with a List EPC7 amplifier (Medical Systems, Greenvale, NY) and stored on a videocassette recorder (Sony Betamax) equipped with a modified digital audioprocessor [Sony PCM 501ES (Unitrade, Philadelphia)]. Recordings were filtered at 2 kHz, with an eight-pole-Bessel low-pass filter (Frequency Devices, Haverhill, MA), and digitized at 100 μs per point using an INDEC-L-11/73-70 microcomputer system (INDEC, Sunnyvale, CA), unless otherwise indicated. Channel open and closed conductance states were discriminated as described (37, 38). γ was calculated from Gaussian fits to conductance histograms (Fig. 2); open and closed channel lifetimes (τ_o and τ_c, respectively) were determined from exponential fits to probability density distributions of dwell times in the open and closed state (37, 38).

Molecular Models of the Pore-Forming Structure. Structures were optimized by using the CHARMM program package version 19 with modified version 18 parameters (39). A distance-dependent dielectric model was used ($\varepsilon = r$), the array was constrained to C_5 symmetry, and ϕ, ψ values were constrained to (−45°, −60°) with a force constant of 200 kcal/mol per radian^2 (1 kcal = 4.18 kJ). Optimization consisted of minimization, 20-ps molecular dynamics at 300 K, 9-ps dynamics cooling to near 0 K, and reminimization.

EXPERIMENTAL RESULTS AND DISCUSSION

Channel Formation by a Synthetic 23-mer Peptide That Mimics the Sequence of the Putative M2 Transmembrane Segment of the *Torpedo* AcChoR δ Subunit. M2 δ mimicking peptide forms discrete ionic channels when incorporated into lipid bilayers formed either across apertures in non-polar Teflon septi (Fig. 2*A*) or at the tip of glass pipets (Fig. 3*A*) by simultaneous assembly from mixed peptide–lipid monolayers. Single channels with γ = 40 pS are readily detected when bilayers are assembled from peptide–lipid monolayers at 1/1000 peptide/lipid molar ratios (Figs. 2*A* and 3*A*). The superiority in signal-to-noise ratio and time resolution of the single channel recordings obtained from bilayers formed at the tip of pipets is evident. The equivalence of channel properties in the two bilayer modalities validates the notion that the peptide and not the bilayer support determines the

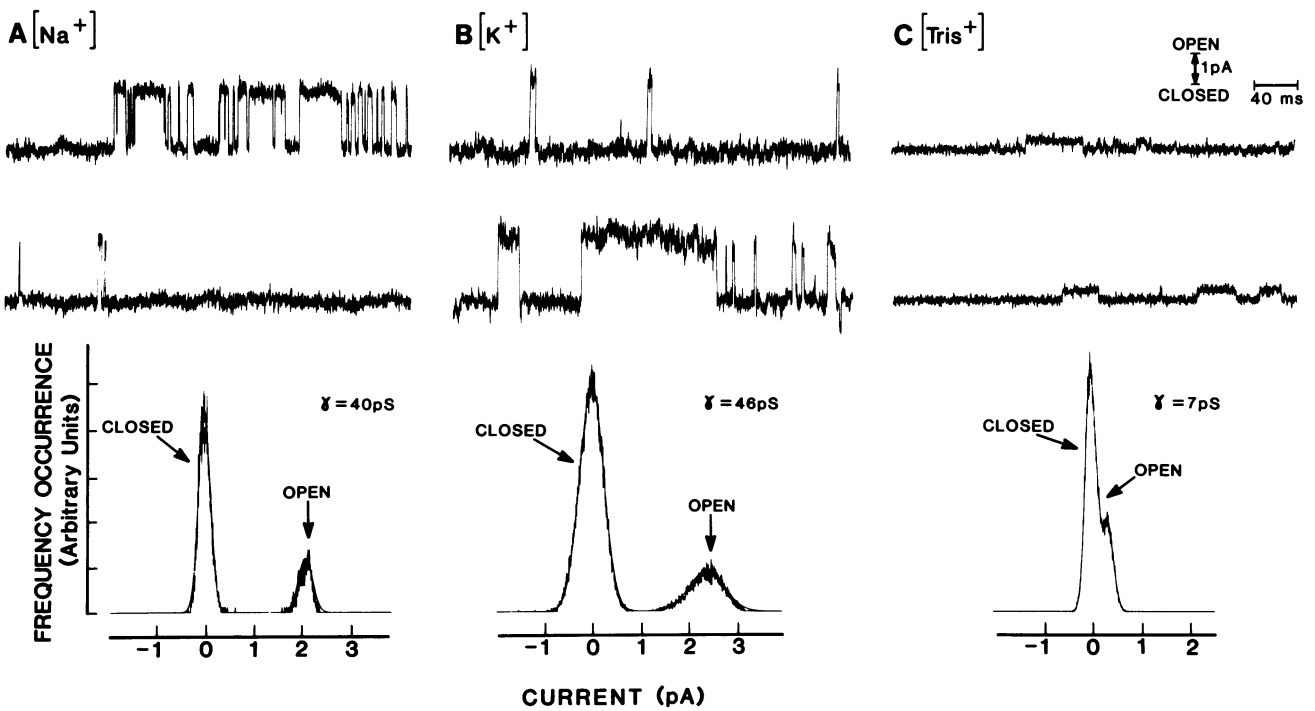

FIG. 3. Single channel currents in membranes containing M2 δ-mimicking peptide and recorded at V = 50 mV in symmetric 0.5 M NaCl (*A*), KCl (*B*), and Tris·HCl (*C*) at pH 7.2. Single channel current histograms are shown under the respective records. Fitted Gaussian distributions (smooth curves) correspond to channel closed state (peak at zero current) and open state [peaks at 2.0 pA (*A*), 2.3 pA (*B*), and 0.35 pA (*C*)]. Calculated γs are γ_{Na^+} = 40 pS, γ_{K^+} = 46 pS, and γ_{Tris^+} = 7 pS.

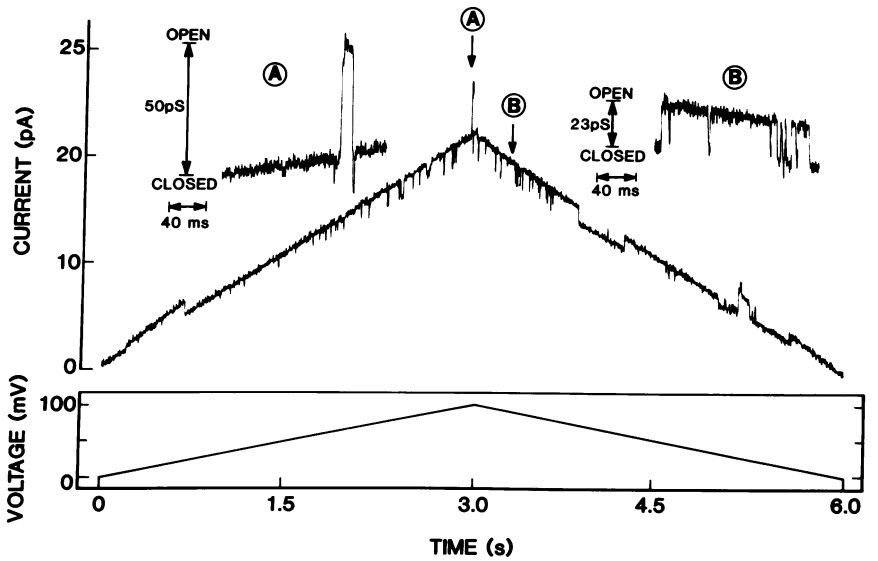

FIG. 4. Synthetic channel peptide conductance is ohmic and heterogeneous. Current records in response to a continuously cycled voltage from 0 to 100 mV in symmetric 0.5 M KCl/5 mM Hepes, pH 7.2. Signals were low-pass filtered at 1 kHz. Sections indicated by arrows (A and B) are displayed at high resolution (note different conductance and time calibrations). Bilayer resistance was 6 GΩ.

channel properties. Therefore, in the description that follows no distinction is made with respect to the specific modality used.

A Synthetic Peptide That Mimics the Sequence of the Putative M1 Transmembrane Segment of the *Torpedo* AcChoR δ Subunit Does Not Form Channels. To address the specificity of channel formation by synthetic peptides, control experiments were done with a 23-mer peptide that mimics a very hydrophobic transmembrane segment of the *Torpedo* AcChoR δ subunit, identified as M1 with sequence Leu-Phe-Tyr-Val-Ile-Asn-Phe-Ile-Thr-Pro-Cys-Val-Leu-Ile-Ser-Phe-Leu-Ala-Ser-Leu-Ala-Phe-Tyr corresponding to residues 226–248 (4–8). M1 δ-mimicking peptide did not elicit discrete current transitions (Fig. 2*B*); solely irregular and erratic conductance fluctuations appeared. Clearly, the M1 δ peptide mimetic interacts with bilayers but does not generate defined conductive pathways, whereas the M2 δ-like peptide produces the discrete conductance events that are characteristic of authentic channel proteins. This is significant because synthetic peptides of variable sequence form channels in lipid bilayers (40–42).

Properties of the Channels Formed by the M2 δ-Mimicking Peptide. *Ionic conduction.* As shown in Fig. 3, single channel currents are well fitted by the sum of two Gaussian distributions corresponding to the closed and open channel states. $\gamma = 40$ pS, 46 pS, and 7 pS in symmetric 0.5 M NaCl (Fig. 3*A*), KCl (Fig. 3*B*), or Tris·HCl (Fig. 3*C*), respectively. The conductance selectivity ratio is Na^+: K^+: $Tris^+$ = 1.0:1.2:0.18. The percentage of time that the channel is open, as determined from the area under each Gaussian, is 20%, 20%, and 30% for Na^+, K^+, and $Tris^+$, respectively.

Ionic selectivity. The channel is cation selective as determined from reversal potential measurements under single salt concentration gradients of either NaCl or KCl: the transference number for cations, t^+, was ≥0.97. The ionic selectivity sequence, as inferred from the ratio of γ in symmetric solutions of NaCl, KCl, and Tris·HCl is $K^+ > Na^+ > Tris^+ >> Cl^-$.

Channel gating kinetics. The synthetic channel shows ohmic behavior with random openings and closings occurring along the V range between 0 and 100 mV as illustrated in Fig. 4. The membrane contained a channel with γ = 23 pS that underwent frequent transitions between open and closed states (arrow B) and a larger channel with γ = 50 pS that opened briefly and sporadically (arrow A). The occurrence of openings with distinct γ amplitudes and variable open and closed lifetimes is a conspicuous feature of single channel recordings obtained with M2 δ-mimicking peptide in symmetric solutions of NaCl, KCl, and Tris·HCl. Histograms of dwell times in open and closed states for the distinct conductance events are well fitted by a single exponential. Channel lifetimes for open (τ_o) and closed (τ_c) states are in the millisecond time range. Results of such analysis are summa-

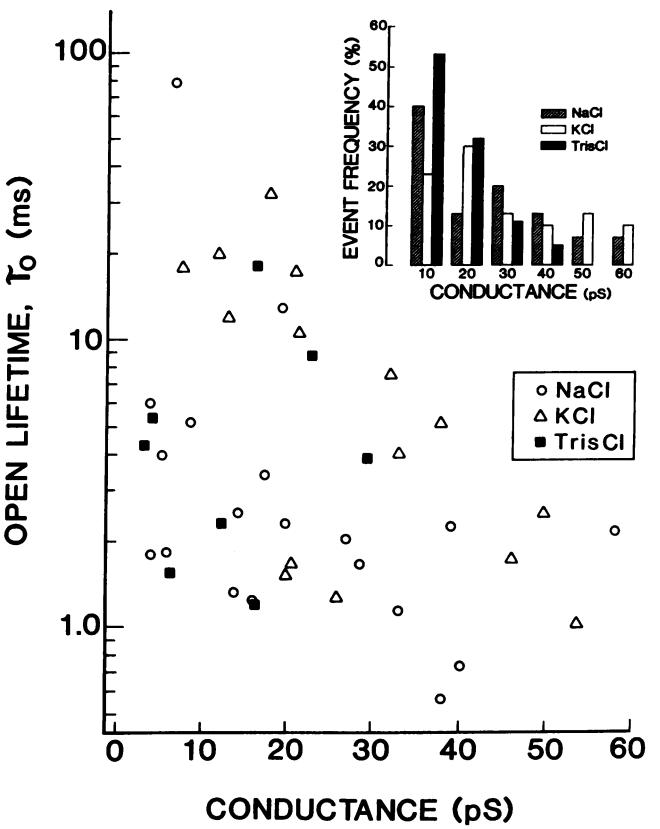

FIG. 5. Relationship between distinct conductances and corresponding channel open lifetimes in symmetric NaCl, KCl, and Tris·HCl. Data were filtered at 2 kHz and the contribution of short events (≤200 μs) was systematically disregarded. (*Inset*) Relative frequency of occurrence of distinct conductances (i.e., % of total number of membranes that exhibit a given γ) in Na^+, K^+, and $Tris^+$. Data collected from 79 membranes formed at the tip of patch pipets are summarized. The total number of events analyzed was 8588 (30 membranes), 6436 (30 membranes), and 3982 (19 membranes) for Na^+, K^+, and $Tris^+$, respectively. Note that the scale for τ_o is logarithmic. Other conditions were as for Fig. 3.

rized in Fig. 5. In general, smaller conductances tend to exhibit longer τ_o, whereas larger events ($\gamma \geq 50$ pS) appear in brief bursts of openings. Furthermore, the frequency of occurrence of distinct conductance events decreases as γ increases (Fig. 5 *Inset*).

The Heterogeneity of Channel Conductance and Lifetime Suggests a Self-Assembled Oligomer as the Underlying Structure. The heterogeneous distribution of γ and τ_o and the sharp decline of the frequency of occurrences and τ_o with increments in γ (Fig. 5) provide a clue to the nature of the structures underlying the observables. We conjecture that the channel recorded in bilayers results from a noncovalently bonded oligomer that self-assembles in the membrane to acquire a minimum energy configuration. Smaller oligomers should have lower γ and their higher frequency of occurrence suggests that they are more stable than larger arrays. As the size of the oligomer increases, γ increases but τ_o decreases. These general features are displayed in Na^+, K^+, or $Tris^+$ (Fig. 5); however, there are specific differences worthy of mention. Consider first Na^+ and K^+: Conductance events are distributed between 5 pS $\leq \gamma \leq$ 65 pS. In contrast, no events with $\gamma \geq 40$ pS were detected in $Tris^+$. In keeping with the AcChoR subunit stoichiometry (1) and sequence (2–8) and emphasizing the similar γ, τ_o, and τ_c of synthetic peptide and purified authentic *Torpedo* AcChoR channel (γ = 45 pS, $\tau_o \approx 4$ ms, $\tau_c \approx 2$ ms) under identical conditions (37, 38), it is tempting to suggest that the channels recorded in Na^+ with $\gamma = 40$ pS, $\tau_o = 2.2$ ms, and $\tau_c = 3.0$ ms (Figs. 2*A* and 3*A*) and in K^+ with $\gamma = 46$ pS, $\tau_o = 1.7$ ms, and $\tau_c = 1.5$ ms (Fig. 3*B*) arise from a bundle of five parallel α-helices. Considering an interaxial helical distance of 9 Å, as inferred from crystallographic data of soluble proteins that exhibit a bundle structure of parallel helices (43, 44), a pore area of 44 Å^2 is calculated for a pentameric array. Such a value is compatible with the estimated AcChoR pore size as inferred from electrophysiological measurements (21–24). We note, however, that other conductance species measured in bilayers may correspond to smaller or larger peptide oligomers.

We selected $Tris^+$ as a permeant cation (Figs. 3*C* and 5) because of its critical properties: (*i*) $Tris^+$ passes through authentic AcChoR channel with a permeability ratio, P, relative to Na^+, $P_{Tris^+}/P_{Na^+} = 0.18$ (23); (*ii*) the molecular dimensions of $Tris^+$, as estimated from Corey–Pauling–Koltun models (45), are 6.0 Å × 6.9 Å × 7.7 Å. Thus, pores narrower than this cross section (≈46 Å^2) would not allow current flow in symmetric $Tris^+$ solutions where $Tris^+$ is the current-carrying species. This cut-off size suggests that pentamers and larger oligomers may be responsible for the single channel currents recorded in $Tris^+$ (Figs. 3*C* and 5) because a tetrameric array would generate a pore area ≈ 16 Å^2 at an interhelical distance of 9 Å. Conductance events with $\gamma = 7$ pS, $\tau_o = 1.5$ ms, and $\tau_c = 1.0$ ms displayed in Fig. 3*C* were selected because they are the most abundant (Fig. 5) and exhibit comparable τ_o and τ_c to those in Na^+ and K^+. Assuming that the gating kinetic properties of the channel peptide are equivalent in chloride solutions of Na^+, K^+, and $Tris^+$, this putative pentameric channel has an apparent ionic selectivity sequence of $K^+ > Na^+ > Tris^+ >> Cl^-$, which is comparable to that characteristic of the authentic AcChoR (21–24, 37). This is summarized in Table 1. In contrast, a peptide channel designed to mimic a putative channel-forming segment of the voltage-dependent sodium channel (Sc_1; ref. 35) does not emulate the properties of the AcChoR ion-conductive pathway (Table 1). This result supports the reliability of the approach insofar as it relieves concerns arising from nonspecific perturbations of bilayers induced by some peptides and other surfactants.

Table 1. Ionic conduction characteristics of authentic AcChoR and sodium channel proteins and of corresponding synthetic channel peptides

Property	*Torpedo* AcChoR*	M2 δ peptide†	Sodium channel‡	Sc_1 peptide§
γNa^+, pS	45	40	25	20
$\gamma K^+/\gamma Na^+$	1.1	1.2	0.13	1.0
$\gamma Tris^+/\gamma Na^+$	0.18	0.18	ND	ND
$\gamma Cl^-/\gamma Na^+$	≤0.01	≤0.03	<0.01	≤0.1

ND, not determined.
*Determined in symmetric 0.5 M NaCl, KCl, and Tris·HCl and from reversal potential measurements of *Torpedo* AcChoR (ref. 37; unpublished results).
†Refers to the most frequent event, as described in this work.
‡Determined in symmetric 0.5 M NaCl and KCl and from reversal potential measurements of batrachotoxin-modified sodium channels from rat brain (46).
§Refers to the most frequent event, determined in symmetric 0.5 M NaCl and KCl and from reversal potential measurements (35).

Molecular Modeling of the Pore-Forming Structure. Previous modeling for the sodium channel protein showed that aligned, regular peptide helices can form noncovalent com-

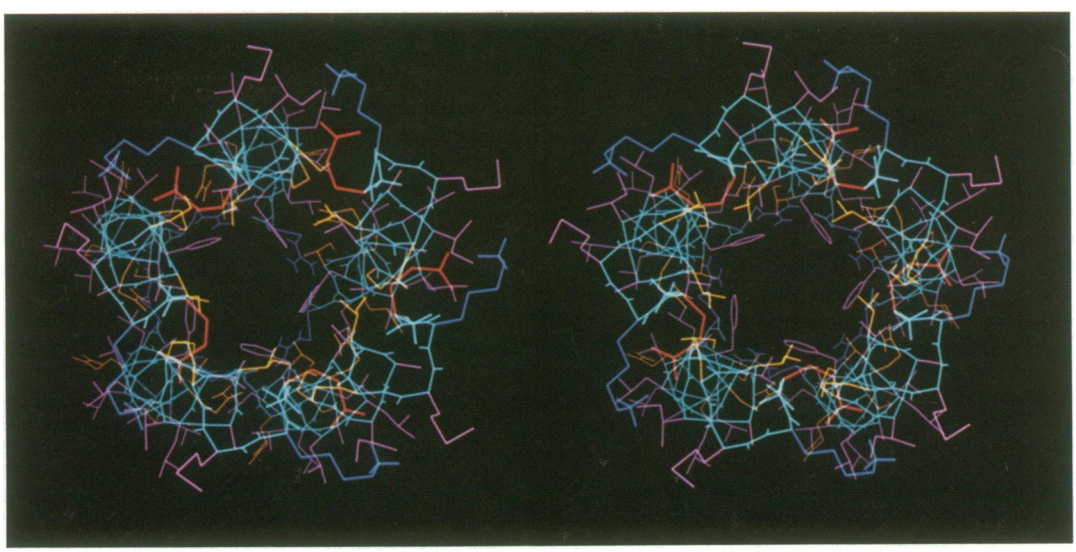

FIG. 6. Stereo, end view of pentameric C_5-symmetric array of the 23-mer synthetic peptide. The N terminus is in the front and is assigned to the extracellular face of the membrane. The α-carbon backbone of the five helices is shown in light blue. Amino acid side chains are colored by functional type: basic, blue; acidic, red; polar-neutral, orange; and lipophilic, violet. The lowest energy structure shown has S8 facing the lumen of the pore.

plexes with a central pore (35, 47, 48). The 23-mer peptide of this study was placed in a pentameric, C_5-symmetric, parallel array using the previous tetrameric sodium channel model as a template. Peptide side chains were adjusted by means of interactive molecular graphics to avoid short steric contacts. The pentameric array was then optimized using energy minimization and molecular dynamics with constraints to maintain C_5 symmetry and backbone torsions characteristic of a regular α-helix (39). Four initial orientations differing by successive rotations of 100° about the axis of an individual helix were tested. Subsequently, four additional orientations were obtained from the lowest energy structure of the first set by rotating each helix ±100° or ±200° about its axis. Two structures were calculated to be at least 10% more stable than the other six, whose energy was about −200 kcal/mol per peptide chain. One low-energy structure was not considered further because S8 was on the outside (contrary to chemical labeling experiments) and the pore had a diameter <2 Å at its narrowest point (Q13). From the eight independent optimizations, the lowest energy structure shown in Fig. 6 was chosen as the most plausible model for the channel formed by the synthetic peptide.

The pentameric array of the model channel has an internal pore with a diameter ranging from ≈4 Å at its narrowest point to ≈6 Å at its widest extent. Nonpolar residues are predominantly on the outside and polar residues are predominantly on the inside, except at the two ends of the helices. Residues S4, T5, S8, A12, F16, and T20 face the lumen of the pore. The R23 side chains bridge the C termini of neighboring helices forming a ring at one end of the pore. At the other end, E1 bridges the amino groups of the N terminus and K2 within each helix. This symmetric pentamer conforms to the general features of the packing arrangement postulated for the $\alpha_2\beta\gamma\delta$ pentamer (2, 3, 9–11, 14–19). The outside is lipophilic, the inside is more hydrophilic, and S8 (corresponding to S262 of the AcChoR δ subunit) is exposed on the channel lumen in accord with chemical labeling experiments.

The valuable collaborations of T. Gabriel and J. Tomich are gratefully acknowledged.

1. Reynolds, J. & Karlin, A. (1978) *Biochemistry* **17,** 2035–2038.
2. Stroud, R. M. & Finer-Moore, J. (1985) *Annu. Rev. Cell. Biol.* **1,** 369–401.
3. Heinemann, S., Asouline, G., Ballivet, M., Boulter, J., Connoly, J., Deneris, E., Evans, K., Evans, S., Forrest, J., Gardner, P., Goldman, D., Kochhar, A., Luyten, W., Mason, P., Treco, D., Wada, K. & Patrick, J. (1987) in *Molecular Neurobiology: Recombinant DNA Approaches*, eds. Heinemann, S. & Patrick, J. (Plenum, New York), pp. 45–96.
4. Noda, M., Takahashi, H., Tanabe, T., Toyosato, M., Furutani, Y., Hirose, T., Asai, M., Takashima, H., Inayama, S., Miyata, T. & Numa, S. (1982) *Nature (London)* **299,** 793–797.
5. Noda, M., Takahashi, H., Tanabe, T., Toyosato, M., Kikyotani, S., Hirose, T., Asai, M., Takashima, H., Inayama, S., Miyata, T. & Numa, S. (1983) *Nature (London)* **301,** 251–255.
6. Noda, M., Takahashi, H., Tanabe, T., Toyosato, M., Kikyotani, S., Furutani, Y., Hirose, T., Takashima, H., Inayama, S., Miyata, T. & Numa, S. (1983) *Nature (London)* **302,** 528–532.
7. Claudio, T., Ballivet, J., Patrick, S. & Heinemann, S. (1983) *Proc. Natl. Acad. Sci. USA* **80,** 1111–1115.
8. Devillers-Thiery, A., Giraudat, J., Bentaboulet, M. & Changeux, J. P. (1983) *Proc. Natl. Acad. Sci. USA* **80,** 2067–2071.
9. Guy, H. R. (1984) *Biophys. J.* **45,** 249–261.
10. Guy, H. R. (1986) in *Nicotinic Acetylcholine Receptor Structure and Function*, NATO Advanced Study Institute Series H3, ed. Maelicke, A. (Springer, New York), pp. 447–463.
11. Finer-Moore, J. & Stroud, R. M. (1984) *Proc. Natl. Acad. Sci. USA* **81,** 155–159.
12. Lindstrom, J. (1986) *Trends NeuroSci.* **9,** 401–407.
13. Ratnam, M., LeNguyen, D., Rivier, J., Sargent, P. B. & Lindstrom, J. (1986) *Biochemistry* **25,** 2633–2643.
14. Giraudat, J., Dennis, M., Heidmann, T., Chang, J.-Y. & Changeux, J. P. (1986) *Proc. Natl. Acad. Sci. USA* **83,** 2719–2723.
15. Changeux, J. P., Pinset, C. & Ribera, A. (1986) *J. Physiol. (London)* **378,** 497–513.
16. Changeux, J. P. & Revah, F. (1987) *Trends NeuroSci.* **10,** 245–250.
17. Oberthür, W. & Hucho, F. (1988) *J. Protein Chem.* **7,** 141–150.
18. Hucho, F., Oberthür, W. & Lottspeich, F. (1986) *FEBS Lett.* **205,** 137–142.
19. Guy, H. R. & Hucho, F. (1987) *Trends NeuroSci.* **10,** 318–321.
20. Imoto, K., Methfesssel, C., Sakmann, B., Mishina, M., Mori, Y., Konno, T., Fukuda, K., Kurasaki, M., Bujo, H., Fujita, Y. & Numa, S. (1986) *Nature (London)* **324,** 670–674.
21. Dani, J. A. & Eisenman, G. (1987) *J. Gen. Physiol.* **89,** 959–983.
22. Adams, D. J., Dwyer, T. M. & Hille, B. (1980) *J. Gen. Physiol.* **75,** 493–510.
23. Dwyer, T. M., Adams, D. J. & Hille, B. (1980) *J. Gen. Physiol.* **75,** 469–492.
24. Lewis, C. A. & Stevens, C. F. (1983) *Proc. Natl. Acad. Sci. USA* **80,** 6110–6113.
25. Nef, P., Mauron, A., Stalder, R., Alliod, C. & Ballivet, M. (1984) *Proc. Natl. Acad. Sci. USA* **81,** 7975–7979.
26. Polla, R. J., Mixter-Mayne, K. & Davidson, N. (1984) *Proc. Natl. Acad. Sci. USA* **81,** 7970–7974.
27. Kubo, T., Noda, M., Takai, T., Tanabe, T., Kayano, T., Shimizu, S., Tanaka, K., Takahashi, H., Hirose, T., Inayama, S., Kikuno, R., Miyata, T. & Numa, S. (1985) *Eur. J. Biochem.* **149,** 5–13.
28. Garnier, J., Osguthorpe, D. J. & Robson, B. (1978) *J. Mol. Biol.* **120,** 97–120.
29. Chou, P. Y. & Fasman, G. D. (1978) *Adv. Enzymol.* **47,** 45–148.
30. Schiffer, M. & Edmundson, A. B. (1967) *Biophys. J.* **7,** 121–135.
31. Kaiser, E. T. (1987) *Trends Biochem. Sci.* **12,** 305–309.
32. Eisenberg, D., Schwarz, E., Komaromy, M. & Wall, R. (1984) *J. Mol. Biol.* **179,** 125–143.
33. Barany, G. & Merrifield, R. B. (1980) in *The Peptides: Analysis, Synthesis, Biology*, eds. Gross, E. & Meienhofer, J. (Academic, New York), Vol. 2, pp. 1–255.
34. Tam, J. P., Heath, W. F. & Merrifield, R. B. (1983) *J. Am. Chem. Soc.* **105,** 6442–6445.
35. Oiki, S., Danho, W. & Montal, M. (1988) *Proc. Natl. Acad. Sci. USA* **85,** 2393–2397.
36. Oiki, S., Danho, W. & Montal, M. (1988) *Biophys. J.* **53,** 636 (abstr.).
37. Montal, M., Anholt, R. & Labarca, P. (1986) in *Ion Channel Reconstitution*, ed. Miller, C. (Plenum, New York), pp. 157–204.
38. Labarca, P., Rice, J. A., Fredkin, D. R. & Montal, M. (1985) *Biophys. J.* **47,** 469–478.
39. Brooks, B. R., Bruccoleri, R. E., Olafson, B. D., States, D. J., Swaminathan, S. & Karplus, M. (1983) *J. Comp. Chem.* **4,** 187–217.
40. Molle, G., Dugast, J. Y., Duclohier, H., Daumas, P. & Spach, G. (1988) *Biophys. J.* **53,** 193–203.
41. Tosteson, M. T., Capora, L. & Tosteson, D. C. (1988) *Biophys. J.* **53,** 9 (abstr.).
42. Lear, J. D., Wasserman, Z. R. & DeGrado, W. F. (1988) *Science* **240,** 1177–1181.
43. Weber, P. C. & Salemme, F. R. (1980) *Nature (London)* **287,** 82–84.
44. Chothia, C., Levitt, M. & Richardson, D. (1981) *J. Mol. Biol.* **145,** 215–250.
45. Huang, L.-Y. M., Catterall, W. A. & Ehrenstein, G. (1978) *J. Gen. Physiol.* **71,** 397–410.
46. Hartshorne, R. P., Tamkun, M. & Montal, M. (1986) in *Ion Channel Reconstitution*, ed. Miller, C. (Plenum, New York), pp. 337–362.
47. Greenblatt, R. E., Blatt, Y. & Montal, M. (1985) *FEBS Lett.* **193,** 125–134.
48. Madison, V., Berkovitch-Yellin, Z., Fry, D., Greeley, D. & Toome, V. (1988) in *Synthetic Peptides: Approaches to Biological Problems*, UCLA Symposia on Molecular and Cellular Biology, New Series, eds. Tam, J. & Kaiser, E. T. (Liss, New York), Vol. 86, in press.